On the Low-Level Wind Structure of Tropical Storms

by

Lawrence A. Hughes

University of Chicago

ABSTRACT

A number of reconnaissance flights into large Pacific tropical cyclones are combined to obtain a generalized pattern of winds at low level (about 1000 feet) under both stationary and non-stationary conditions. Using these winds, a number of dependent computations are made including relative trajectories, divergence, vertical motion, rainfall, energy, and relative vorticity.

1. Introduction

Up to World War II, nearly all of the data available for the study of the wind distribution in tropical storms were obtained from time sections of wind direction and speed for island and coastal stations. Since 1943, however, the military services of the United States have undertaken aerial reconnaissance of these storms in ever increasing number. It is the purpose of this report to use the observations taken on these flights to extend our knowledge on the wind structure of tropical storms.

2. Material used and plotting techniques

The data studied covers the period 1945-47. Observations taken during flights made in 1945 were obtained from Navy synoptic charts, those for 1946 and 1947 from Navy publications of the operations of Meteorological Squadron One in the Pacific and Meteorological Squadron Three in the Atlantic. During the flights, the observations were made at relatively short time intervals, usually 15 minutes, while the aircraft was flying at an altitude of about 1000 feet in and around the storm circulation. From the fairly large number of flights available, only those that entered the eye or circumnavigated the storm were selected since treatment of the data necessitated a good knowledge of the position of the storm center. Of the 84 flights finally chosen from some 28 storms, one-third entered the eye and another one-third gave an estimated position of the center. The location of the remaining centers, as well as a check on the given centers, was obtained from composite storm tracks.

Because the time interval between the first and last observations was frequently up to six hours, the observations were not considered to be synchronous but were adjusted to allow for storm movement. To accomplish this, the speed and direction of movement of the storm were obtained from the storm tracks and the position of each observation was adjusted relative to the time the aircraft was nearest to or entered the eye. After this adjustment, the observations were replotted on ordinary graph paper, which was considered to be a section of a map.

3. Analysis techniques

The original intent had been to analyze individual flights, but the paucity of data made unique solutions impossible, and it was decided to compute the average wind distribution by combining storms. While the method initially chosen would bring out the individual peculiarities of storms, combination yields a more generalized wind distribution upon which these peculiarities are superimposed.

Due to variations in storm size and stage of maturity, subclassification was essential prior to combination. A frequency distribution of storm size revealed a bimodal distribution with two distinct classes, namely storms whose total circulation was less than and greater than 780 km in radius. The larger storms, since all were in the mature stage of development and all were situated in the Pacific, were more homogeneous. While further discussion will be confined to this group, it may be added that the wind distributions obtained for the small storms were very similar to those for the large storms as presented here. The differences were mainly in the size of the overall circulation and in the area covered by a particular wind regime rather than in intensity or relative distribution of the winds.

The data for the large storms were taken on 60 of the flights into 13 different storms and consist of about 500 individual wind reports. Since most of the flights selected followed a more or less spiral path into or near the storm center and a spiral path back out, the distribution of the wind reports was remarkably uniform throughout the storm region from 0.5[illegible] to 3 radii from the center. The actual combination of this data was accomplished by first dividing each storm into octants oriented with respect to the direction of motion of the storms. A graph of wind speed vs. distance from the storm center was made for each octant by plotting the appropriate data from all of the storms on each graph. The number of points per graph was then increased by combining the octants to form overlapping quadrants, that is, octants 1 and 2 were combined, 2 and 3 combined, etc. A wind profile for each of the overlapping quadrants was obtained from the graphs by drawing a free-hand fit to the data then adjusting this curve so that the sum of the deviations of the individual points approached zero. While the use of overlapping quadrants might have introduced some false symmetry into the storm, it added considerable reliability to the velocity profiles.

The radial and tangential components of each wind report were computed relative to a system of polar coordinates with the storm center as the origin. Each of these components was treated as described above for the total wind. Since we now have three curves for each quadrant, any two of which uniquely determine the third, a consistency check is in order.

While the individual values of the mean deviation for the 24 curves ranged from 9 to 13 knots, expressing the uncertainties inherent in observations of this type and the variation between storms, only minor adjustment of the total and/or tangential velocity curves was necessary to obtain internal consistency. This alone suggests reliable results, and since it is believed that the final curves were drawn with sufficient data, are close to the best fit for the data, and are internally consist-

ent as well, they should be representative as a mean for this group of storms. As this would not be true of the region within 0.5° lat of the storm center since too few observations occurred there and the errors due to uncertain storm centering could be large, the curves were not extended into this region.

4. Stationary storms

Five of the above flights, consisting of about 50 wind reports, were made in a storm which was practically stationary. These had to be treated somewhat differently as a direction of motion, and therewith octants, could not be defined. They were combined by considering all of the observations in making the single set of velocity profiles shown in Figure 1.

Profiles of this type are frequently expressed by an equation of the form vr^x equals c, where v is the wind speed, r is the distance from the storm center, c and x are constants. Such an expression is certainly most appropriate for the stationary case where symmetry is more probable and where the existence of asymmetry cannot be verified because of the method of combination employed. The value of x was computed from the tangential velocity profile by insertion in the equation of the values of v and r taken from points 1° and 3° lat from the storm center. The figure x = 0.62 thus obtained was used to compute a profile. This profile agreed quite well with the profile presented except for the region within 1° lat of the storm center. Here the computed values became progressively larger than the actual values as the center of the storm was approached. The value 0.62 agrees well with the 0.5 often mentioned in the literature (for example Byers (1)) as fitting observation, especially when one considers that the latter figure usually is applied to the inner portions of the storm, i.e., within 2° lat of the center. The deviation of the actual values from the computed in this inner region indicate use of a figure somewhat less than 0.62 for this region alone. On the other hand, the figure of 1.0 as found in the well-known simple vr vortex would be approached if only the outer portion of the storm were considered.

Values for divergence and vorticity computed from Figure 1 are given in Figure 2. The method of computation is discussed in a later section. Reference to both Figures 1 and 2 will show that in spite of a radial component directed inward, divergence exists to within almost 1.5° lat of the storm center. It is quite possible that this region, i.e., where the divergence shifts over to convergence, is the region of the bar of the storm as described by Byers and others. For it is here that the intense convergence, and therewith upward motion, necessary to produce the solid mass of cumulonimbus known as the bar is first found.

5. Moving storms

Basic distributions of the winds. Field distributions of the total wind speed and its components were determined for the moving storms by the selection of values from the adjusted velocity profiles described earlier and plotting them in their respective positions on a map grid. Figure 3 gives the distribution of the total wind speed resulting from such a procedure after drawing isotachs. Since the velocity profiles only extended to within 0.5° lat of the storm center, the innermost isotachs and particularly the gradient around the eye are unsubstantiated. The location and magnitude of the

maximum in the right rear quadrant is definitely shown by the data, however. Such a distribution was expected and is supported by both Cline's study of Caribbean cyclones (2) and Deppermann's study of Philippine typhoons (3). It is rather remarkable however that a maximum greater than 90 knots was obtained when one considers the averaging process used to obtain the values. Although this distribution is for large storms in the mature stage of development, one might note the relatively small area of the circulation covered by winds strong enough to be considered typhoon winds, i.e., 65 knots and higher.

Such a pattern of winds could result from the superposition of a uniform basic current on a radially symmetric vortex, for, looking downstream along the current, the current would reinforce the vortex winds to the right and retard those to the left of the vortex center. In an attempt to find the speed of such a basic current, the component of the wind parallel to the direction of movement was determined. Integration of this component over an area approximately 4° lat in radius yielded a value for the current of about half the mean speed of movement (10 knots) of the storms. The value was the same regardless of the radius of the area chosen for integration. While the value determined from the data may be right, some discrepancy in this direction would be expected to result from such a composite picture and from the use of overlapping quadrants. While removal of all the possible discrepancy would affect the individual profiles only a small amount, it would be in a direction that would give a more asymmetric distribution of winds than that indicated.

The tangential and radial components are given in Figures 4 and 5 respectively. The distribution of the tangential component is extremely similar to that of the total wind speed, differing mainly by but five to ten knots in its magnitude.

The incurvature field (angle of inflow) as computed from the wind fields given above is shown in Figure 6. Such a field has been described by Ferrel (4) as resulting from the steady translational motion of a vortex which has a relatively uniform incurvature, which would lead one to deduce that much of the asymmetry in the storm is due to its motion. Observations of Hall (5) and Cline agree with the values in Figure 6 to the extent that they found incurvature to be at a minimum in the front portion of the storm and at a maximum to the rear.

From Figures 5 and 6 it might seem that the air in the left rear quadrant of the storm was approaching the storm center at the most rapid rate, but because of the movement of the storm, this is not the case. To obtain the true picture of inflow, we must subtract the storm movement from the total velocity field and then obtain the radial velocity relative to the moving center (Figure 7). We now see that it is the air in the right front quadrant which is really approaching the center at the most rapid rate.

To obtain a complete picture of the flow relative to the moving center, a set of relative trajectories was constructed (Figure 8). These trajectories indicate that the air from the right front quadrant reaches the center in less time than that from any other sector. For example, the time required for a parcel of air from the right front quadrant to move from a point 4° lat from the center to within 0.5° lat of the center is slightly over 12 hours, whereas a parcel from the left rear quadrant requires nearly twice

that long to cover the same radial distance. The parcels in the rear travel a much greater distance, of course.

Fields of divergence and vertical motion. Using the basic wind data just given, a number of subsidiary computations were made assuming the data to exist in an individual storm. One of the most important of these computations is that of the divergence.

The mean horizontal velocity divergence in any region may be computed from the expression

$$Div_2 V = -\frac{1}{A}\int C_n \, dS,$$

where A is the area over which the divergence is measured and C_n is the wind component normal to the distance S extending along the boundary of A and defined positive inward. The divergence was computed for the eight overlapping quadrants by use of the above formula over areas bounded by circles 0.5° lat apart and by radii 90° apart. The divergence field was approximated by plotting the computed values in the center of the area of computation and then drawing isolines (Figure 9). Divergence is indicated where the values are positive and convergence where they are negative. Since the density is practically constant over the area under consideration, this pattern can also be considered as representing that of horizontal mass divergence.

It should be noted that a large amount of divergence exists here as in the case of the stationary storm. Fully half the storm centered on the right front quadrant is divergent to within 2° lat of the center, with the maximum convergence in the rear of the storm. This would indicate that a rapid transition from fairly clear skies to heavy clouds and rain takes place well in toward the storm center in the forward position of the storm, whereas the rear portions have much more cloudiness. This is often observed to occur, but the data of Deppermann and Cline do not substantiate it, for they found that the greater portion of the rain occurred in the forward portion of the storm. This apparent lack of verification is probably due to the fact that their observations were from land stations where the sudden change in the amount of surface friction as the storm moved from water to land could cause much additional convergence and rainfall.

The location of the bar of the storm can be seen here also, as in the stationary case, being in the region of the strong gradient of the divergence. It might seem odd that the region of divergence is also the region of most rapid inflow relative to the moving storm center. But since the term involving the tangential component is much less important in the divergence than that involving the radial component (see Figures 4 and 5), it is this latter term that governs the distribution of divergence, and v_r must increase inward rapidly to create divergence.

The divergence and vertical motion are closely related through the continuity equation; for the equation states that

$$Div_2 V = -\frac{1}{\rho}\frac{d\rho}{dt} - \frac{\partial \omega}{\partial z}.$$

Under the conditions of temperature and pressure prevailing in tropical storms, the density term would be at least one order of magnitude less than the computed

divergence, at least to within 0.5° lat of the storm center. Then neglecting the density term and integrating the above expression with respect to z we obtain

$$W = -\int_0^z \mathrm{Div}_2 \mathbf{V}\, dz = -\overline{\mathrm{Div}_2 \mathbf{V}}\, \Delta z$$

Since the values of divergence in Figure 9 represent $\mathrm{Div}_2 \mathbf{V} \times 10^5$, they also represent the vertical velocity of the air in cm per second at 1 km when the computed divergence is assumed to be the mean from the surface to that level. Thus this figure also gives the field of vertical motion with negative values indicating upward velocities. It also shows that, in the mean, there is relatively little upward motion to within 2° lat of the storm center but inside this radius it increases very rapidly. The neglect of density changes could cause this computed W to be up to about 10 percent too large.

Rainfall and energy computations: Rainfall, and through it the latent heat release, can also be computed from the basic data.

In a steady state with no loss of moisture from the top of the storm (all low-level moisture influx is precipitated), the amount of rainfall can be computed by equating the flux of moisture (F) through a circle around the storm center to the total rainfall within that area. With the model proposed by Riehl (6) in which most of the outflow takes place above 10 km, the moisture loss from the top of the storm would be less than five percent of the low-level influx if we can neglect the liquid water loss. This is so because the mean specific humidity of the outflow would be less than 1.0 gm per kg even under saturated conditions, while at low level it is at least 16.5 gm per kg. Since the liquid water loss should also be small, we shall consider the rainfall equal to the moisture flux and obtain

$$F = 2\pi r V_r \int q \frac{dp}{g} = \pi r^2 R,$$

and

$$R = \frac{2V_r}{rg}\, \bar{q}\, \Delta p,$$

where R is the amount of rainfall per unit area per unit time, Δp is the layer through which all of the flux takes place, and $\bar{q}$ is the mean value for the specific humidity in that layer. Taking the mean value of v_r at various radii, $\bar{q}$ = 16.5 gm per kg (obtained from the mean hurricane sounding after Schaeht (7)), and Δp = 100 mb (see Riehl), the values of R in cm per day were computed and are given in Table 1, columns 2 and 3. These values are such that if the storm passed directly over a station while moving in a straight line, there would have been a total rainfall of about 11 inches in 48 hours. This appears to be a reasonable value, for Cline found 8 to 10 inches occurring under similar conditons in his Atlantic storms.

Since the rainfall as computed was completely dependent on the radial component of the wind and the divergence was nearly so, the rainfall pattern

should be quite similar to this latter pattern.

Multiplication of the rainfall values by the area, the heat of condensation, and the mechanical equivalent of heat, give the energy release per day as shown in column 1 of Table 1. Longley (8) computed the latent heat release in an Atlantic hurricane using actual precipitation reports. His value of 1.9×10^{26} for a 3° lat radius compares well with the 4.36×10^{26} value in Table 1.

The loss of energy within the storm is much more difficult to evaluate due to the number of factors involved and to the lack of adequate data to calculate them. In an attempt to find the order of magnitude of the energy loss due to surface friction alone, Taylor's form of the frictional force $K \rho V^2$ was used (9). Since the winds at hand are for a level around 1000 ft, a value of K somewhat lower than the .0025 usually found with anemometer-level winds must be used. Assuming a value for K of .0015, multiplying Taylor's expression by V, and then integrating with respect to area and time, we obtain the total energy loss due to surface friction. The value obtained for that portion of the storm within 4° lat of the center amounted to about two per cent of the energy gain for the portion. Of course this figure does not include energy dissipation due to internal or lateral friction. However, it is much less than the 12 per cent given by Riehl as the maximum amount of heat energy that can be converted into kinetic energy. The ratio of energy gain to energy loss, which amounted to 50, compares well with the value of 44 obtained by Horiguti (10) in an Okinawa typhoon.

Vorticity computations. The mean relative vorticity of a region may be expressed as

$$C_r = \frac{1}{A} \oint C_t \, ds,$$

where C_t is the tangential component of the wind along the distance S. Using this expression, the vorticity was computed for the same areas as, and in a manner similar to, the divergence. The result is shown in Figure 10.

The relative vorticity may also be expressed as the sum of a shear and a curvature term. In the case at hand the shear term is negative and quite large, ranging from one-half to four times the value of the Coriolis parameter at the mean latitude of the storms (see Figure 3). The curvature term is positive and the high wind speeds combined with the small radii of curvature make it so large that it is everywhere even greater in absolute value than the shear term. In fact it is just where the shear term has its largest negative value that the relative vorticity has its largest positive value. The relative vorticity as well as the absolute vorticity therefore is everywhere positive.

Using the fields of vorticity and divergence given above, the vorticity equation as given by

$$\frac{1}{C} \frac{dC}{dt} = - \mathrm{Div}_2 V$$

was evaluated along the relative trajectories. The variations in f were taken from the value at 20°N, which was the mean latitude of the storm centers.

Nine computations were made over trajectories which ranged from a fraction of an hour to several hours in length. Most of the computations were in the inner portion of the storm since both the vorticity and divergence fields were ill-defined at the outer regions. All quadrants of the storm were covered. The mean value of the computations gave a result in which the divergence value was about half the value necessary for equality to result from the equation. The individual computations did not deviate from the mean a great deal. Of the terms in the complete vorticity equation which were omitted from the computation, the solenoid term is probably quite close to zero and the vorticity transport term is small so that if the complete equation is to balance, there must be some friction effect operative, the nature of which it is beyond the scope of this paper to determine.

6. Summary

A number of serial reconnaissance flights into large mature tropical storms were combined giving a generalized wind distribution for such storms. The data taken in a stationary storm were treated separately by combining all of the data into a single set of velocity profiles for the total, tangential and radial velocities. The tangential velocity curve, when approximated by an expression of the form vr^x equals c, gave a value for x of 0.62. Divergence and vorticity curves were computed from the wind profiles with the divergence curve having positive values to within 1.5° lat of the storm center and then shifting over to a region of strong convergence which might be associated with the bar of the storm.

For the moving storms a field distribution of each of the components of the wind was possible. The field of total wind speed had a maximum greater than 90 knots situated to the right of the direction of motion when looking downstream along this direction. The pattern in general was supported by observation. The tangential component looked very similar to that of the total wind while the radial component had a pronounced maximum in the rear of the storm. The incurvature field, radial component relative to the moving center, and relative trajectories were constructed. The latter two fields plainly showed that it is the air in the front portion of the storm that is really approaching the storm center at the most rapid rate instead of that in the rear, as one might erroneously gather from the first radial component field. In general it required from 12 to 24 hours for the air to travel, from a point 4° lat from the storm center, along the relative trajectories to within 0.5° lat of the center.

From the basic wind fields for moving storms a number of subsidiary computations were made assuming the data to exist in an individual storm. Included were computations for divergence, vertical motion, rainfall, latent heat release, surface frictional energy dissipation, and vorticity.

The divergence field again showed a large area of divergent flow. Almost half of the storm centered on the right front quadrant is divergent. The region of the bar of the storm is also apparent near the storm center where the gradient of the divergence increases sharply.

The vertical motion field is obtained from the divergence field simply by changing the sign of the divergence values when it is assumed that the divergence is a mean through a 1 km layer and the small variations in density are neglected. Therefore the same deductions would arise from it.

As the distribution of rainfall is also closely associated with the distribution of divergence, these two patterns would be very similar. The amount of rainfall was computed by equating it to the low-level influx of moisture; it was found that if the storm passed directly over a station, about 11 inches of rain would fall in the 48 hours required for passage.

The ratio of the latent heat gain of energy to the frictional loss to the sea surface amounted to 50. The order of magnitude was 10^{26} ergs per day.

The vorticity field had a pattern quite similar to that of the divergence field. The vorticity was everywhere positive because the high wind speeds and small radius of curvature allowed the positive curvature term to be so large that it completely overcame the large negative shear term.

7. Remarks

The foregoing should provide a good picture of the generalized large tropical cyclone in the mature stage of development over the ocean, since all of the preceding calculations are internally consistent and many have been compared with observations in individual storms and with the works of other authors, with favorable results.

When attempting to compare the work of this paper with actual storms, it must be realized that the microstructure of the individual storms and variations between storms were almost entirely averaged out, so that any specific storm might vary considerably, in its details, from the generalized picture presented. These details, however, would be superimposed on this generalized picture and not free of its influence.

In the study of tropical cyclones, as in any other phase of meteorology, there is no substitute for data. Since research on tropical storms must be carried out mainly over the open ocean areas where the storms are free of the complications introduced by land influences, aerial reconnaissance provides practically the only source of information. To enable further study of these storms, so that their individual peculiarities may eventually be known, it is hoped that advances in radar and similar innovations will eventually provide the means for a number of aircraft to observe a single storm at the same time and thereby provide a number of observations at different levels without the averaging process of combination. Such observations, when associated with accurate positioning of the aircraft, reliable observational techniques, radar photographs and detailed narrative summaries from the flight members, would quickly lead to a much fuller understanding of the structure of tropical storms.

Acknowledgments

The writer is indebted to Dr. Herbert Riehl for his suggestion of the topic and for his counsel as research adviser. Thanks are extended to Mr. N. E. La Seur and other members of the Department of Meteorology, University of Chicago, for enlightening discussion; to Mr. Homer Hiser for much of the basic plotting work; and to the staff of the drafting room of the department for the preparation of the drawings.

References

1. Byers, H. R., 1944: General Meteorology, New York, McGraw-Hill Book Co., pp 417-448.

2. Cline, I. M., 1926: Tropical Cyclones, New York, Macmillan.

3. Deppermann, C. E., 1937: Wind and Rainfall Distribution in Selected Philppine Typhoons. Manila, Bureau of Printing.

4. Ferrel, William, 1911: A Popular Treatise on Winds, 2nd ed., New York, pp 303-307.

5. Hall, Maxwell, 1917: West Indies hurricanes as observed in Jamaica, Mon. Wea. Rev., vol. 45, December, pp. 587-588.

6. Riehl, Herbert, 1950: A model of hurricane formation, J. App. Phys., vol. 21, pp. 917-925.

7. Schacht, E. S., 1946: A mean hurricane sounding for the Caribbean area, Bull. Am. Met. Soc., vol. 27, pp. 324-327.

8. Longley, R. W., 1949: On the energy of a hurricane, Bull. Am. Met. Soc. vol. 30, p. 194.

9. Taylor, G. I., 1916: Skin Friction of the wind on the earth's surface, Proc. Roy. Soc., vol. 92, p. 196.

10. Horiguti, Y., 1928: On the typhoon of the Far East, Mem. Imp. Obsv., Kobe, vol. 3.

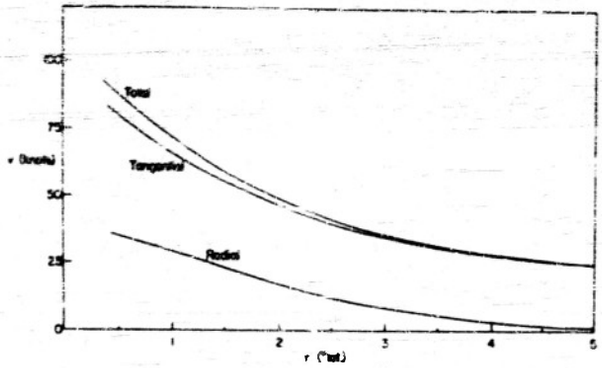

Fig. 1. Velocity profiles in knots. (Stationary case)

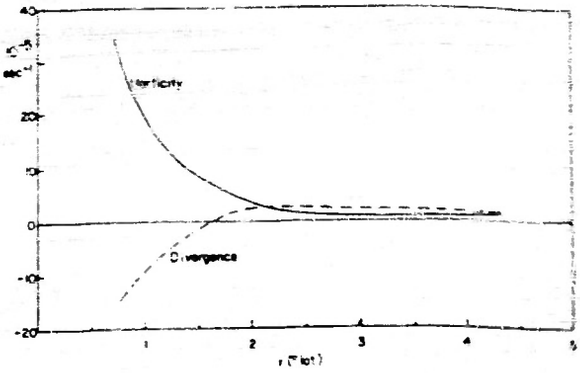

Fig. 2. Divergence and vorticity profiles in units $10^{-5}sec^{-1}$. (Stationary case)

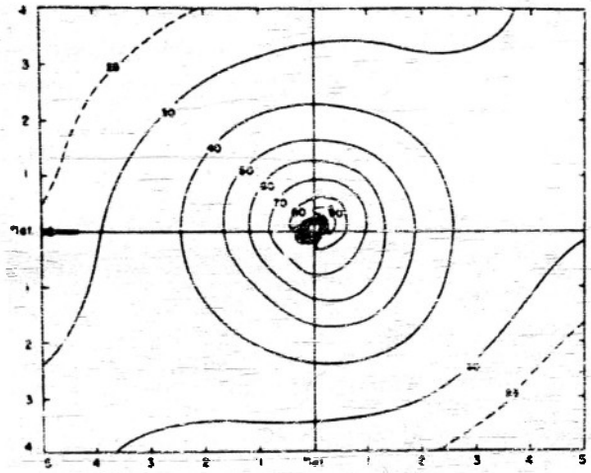

Fig. 3. Total wind speed in knots.*

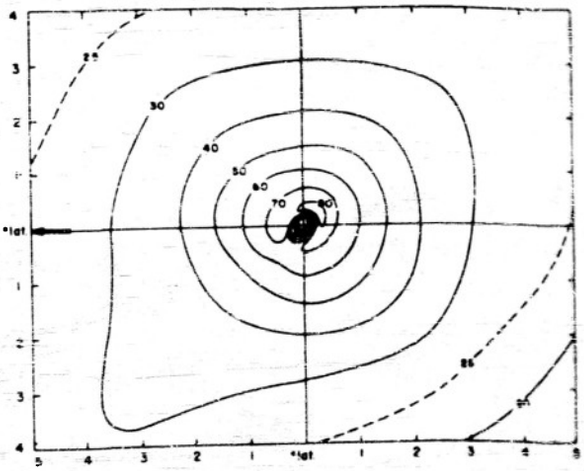

Fig. 4. Tangential velocity in knots.

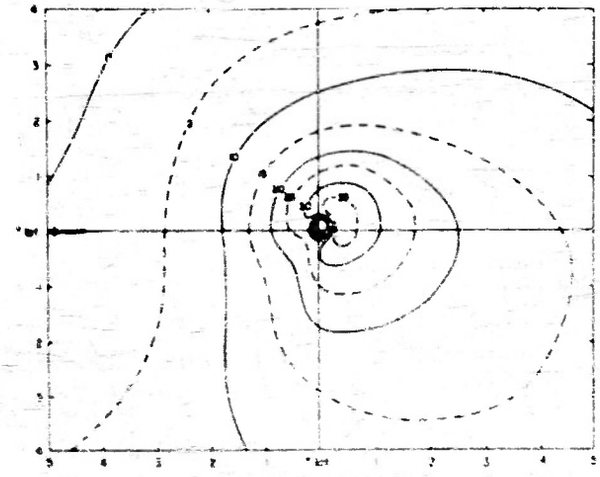

Fig. 5. Radial velocity in knots.

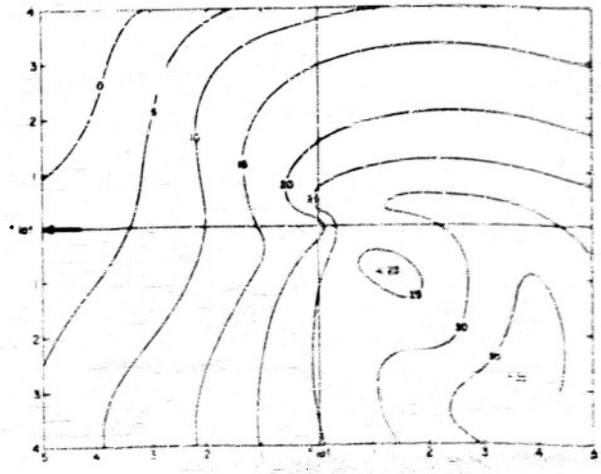

Fig. 6. Incurvature field in degrees.

*In figures 3 through 10, the arrow indicates the direction of storm movement.

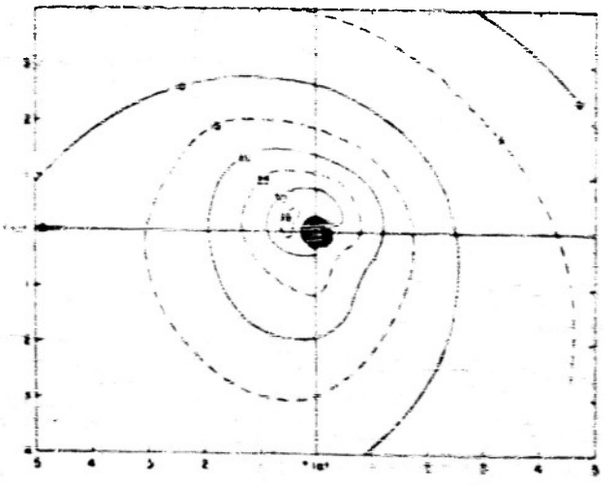

Fig. 7. Radial velocity relative to the moving center (knots).

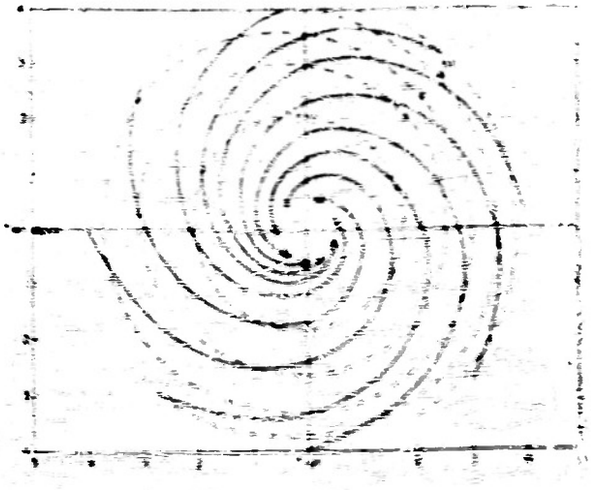

Fig. 8. Trajectories relative to the moving center. Dashed lines indicate hours required to reach 0.5° lat from storm center, by following a trajectory.

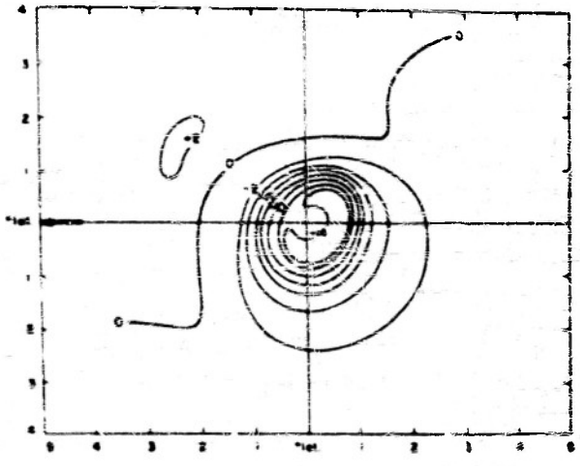

Fig. 9. Divergence field (10^{-5} sec^{-1}). Also vertical motion field in cm sec^{-1} with negative values for upward motion.

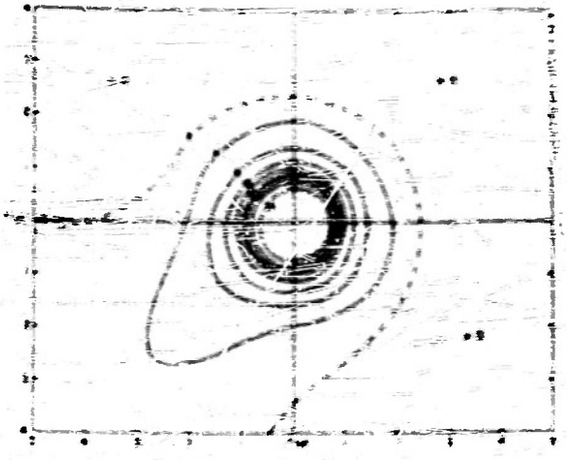

Fig. 10. Relative vorticity field in units 10^{-5} sec^{-1}.

Table I: Rainfall and Energy Values in Moving Storms

Radius °lat	Col 1	Col 2	Ring °lat	Col 3
0.5	210	88.3	0.0-0.5	86.3
1.0	327	33.7	0.5-1.0	18.0
1.5	393	18.0	1.0-1.5	5.4
2.0	419	10.8	1.5-2.0	1.5
2.5	424	7.0	2.0-2.5	0.26
3.0	436	5.0	2.5-3.0	0.46
3.5	462	3.9	3.0-3.5	0.88
4.0	465	3.0	3.5-4.0	0.04

Column headings: Column 1: Total latent heat release inside radius. [10^{24} ergs day^{-1}]
Column 2: Average rainfall inside radius. [cm day^{-1}cm^{-2}]
Column 3: Average rainfall in ring. [cm day^{-1}cm^{-2}]